

Excitation energy dependence of the photoemission spectra of metals

Shyamalendu M. Bose

Department of Physics and Atmospheric Science, Drexel University, Philadelphia, Pennsylvania 19104

Patrick Kiehlm and Pierre Longe

Institut de Physique, Université de Liège, Sart-Tilman, B-4000 Liège, Belgium

(Received 15 November 1979)

The x-ray photoemission spectra (XPS) of simple metals are investigated by using the methods of many-body perturbation theory. Several features of the XPS, such as the infrared catastrophe effect, the effect of intrinsic and extrinsic plasmon production, etc., have previously been considered in different approximations by various authors. In this paper, a unified theory, using a nonseparable core-hole conduction-electron scattering potential, is proposed to describe these features with special attention to the interference effects. The evolution of the shapes of the main line and the first plasmon satellite along with the background is considered as a function of the incident x-ray energy. Numerical results of the intensity and the shape of these lines are presented for Na and Al for the incident photon energies of $5\omega_p$ and $90\omega_p$.

I. INTRODUCTION

In recent years there has been a great deal of interest in both theoretical and experimental studies of the x-ray photoemission spectra (XPS) of metals.¹⁻¹¹ In particular, several papers have appeared on the study of XPS in the ultrasoft-x-ray region.^{8,9} At these low energies (≤ 150 eV), as the energy of the incident x ray varies, the XPS exhibit certain interesting features, e.g., attenuation of the plasmon satellites, variation in the background intensity, as well as the variation in the widths of the main line and the plasmon satellites.

Theoretically the XPS of metals have been treated from several different points of view. The asymmetry in the main line due to the infrared catastrophe has been studied by Doniach and Šunjić² (DS). However, because of the nature of the approximations involved, their theory is valid only very close to the emission edge. The variation in the intensity of the satellites due to quantum interference effects between the intrinsic and extrinsic plasmon excitations has been treated by Chang and Langreth⁴ (CL) and others. In this theory the dispersion and the damping of the plasmon has been neglected. The DS and CL theories are valid in two different energy regions and there is no simple connection between them.

In this paper we propose a unified theory of the XPS of metals, which is valid in both the main line and the plasmon satellite regions. We extend the DS theory by using a realistic potential to describe the core-hole conduction-electron scattering. The satellite intensities are calculated by keeping the dispersion and the attenuation of the plasmon excitations. Another new feature of our

calculation is that from the dynamic part of the effective interaction we also calculate the energy dependence of the background XPS intensity. In short, in this paper we calculate the width and the asymmetry of the main line on one hand and the plasmon satellite and the background on the other hand.

There is a variation in the shape and size of these quantities as a function of the incident x-ray energy. At very low energies of the incident photon (photoelectron energy approaching zero) the situation is similar to the x-ray photoabsorption (XPA) case where the quantum interference term practically cancels the satellite intensity due to both plasmon excitations. In the XPA, the cancellation is so strong that the calculated plasmon structure is negligible, except at the upper limit of the plasmon frequency where a structure of approximately 5% intensity is calculated and observed.¹² A similar cancellation is observed in the low-energy XPS. However, in the XPS, as the incident photon energy becomes large, the interference effect decreases since at these energies the intrinsic and the extrinsic plasmons can be considered to be produced in different spatial regions. At these high energies the distribution of the satellite intensities can be obtained by a classical approach (Poisson theory).⁴ Our unified theory is valid in any photon-energy range and is in agreement asymptotically with the existing theories in the various energy limits.

The effect of electron-electron interaction is calculated in the random-phase approximation (RPA) in the present theory. We limit our attention in the spectral region extending from the main line to the first plasmon satellite. We assume the usual jellium model for describing the motion of

the electron in the metal. The only parameter in the problem is the electron density parameter r_s . Thus, contrary to various other theories, our study can be considered to be an *ab initio* calculation. We will apply our theory to the specific cases of Na with $r_s = 3.993$ and Al with $r_s = 2.0737$.

We consider a simple geometrical situation where the metal is taken to be semi-infinite in extent. We consider those photoelectrons which escape normally from the surface. Our theory, however, can be applied without any major modifications to more complicated situations. For example, this theory can be used to study photoemission at other angles, photoemission in a thin-film metal, and also in the case where the core-hole density would depend on the distance from the surface.

It should be mentioned here that in the present paper we have not included two important effects which may also contribute to the XPS intensity. These are the secondary effects related to the sudden creation of the core hole as well as its finite lifetime (its structure does not play a significant role), and the surface effects due to the surface structures and surface modes. We are aware that there is considerable interest in these problems especially in the surface effects which have been calculated in detail by Chang and Langreth.¹³ These authors have shown that the surface effects become important at lower electron energies, and are comparable to the interference effect even at high energies. However, our aim here is to consider the bulk effects as completely as possible, by using a model with a minimum number of parameters. Thus we calculate the XPS intensity in the jellium model with a sharp surface (the only parameter being r_s). The only role of the metal surface that we consider here is the cutoff of the interaction between the photoelectron and the metal after a time τ , the time needed by the photoelectron to reach the surface after its production inside the metal. However, our theory does not exclude the possibility of further study of the neglected effects in the framework of the present model.

II. FORMALISM

The process of x-ray photoemission in a metal is represented by the diagram in Fig. 1. In this figure the incident photon of energy ω is described by the wavy line. The double line pointing downward represents the propagator of a core hole of energy ϵ_B (negative) created by the ejection of the photoelectron in the core state, and the single line pointing upward indicates the propagator of the photoelectron of energy $\epsilon_k = k^2/2m$, inside the met-

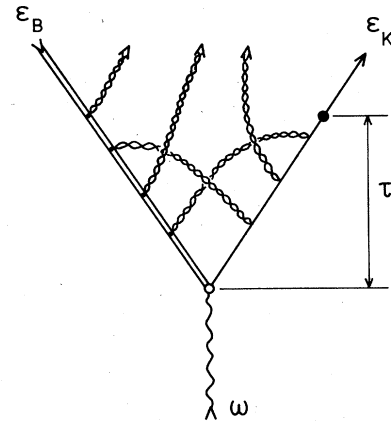


FIG. 1. Diagram representing the x-ray photoemission process accompanied by various (intrinsic, extrinsic, and interference terms) many-body excitations in a metal. The wavy line represents the incident photon of energy ω and the directed double line and single line are the propagators for the core hole and the photoelectron, respectively. The lines of chain represent single-pair and plasmon production.

al. All possible excitations due to many-body effects in the metal are represented by the lines of chain (the RPA effective interaction). The black dot on the photoelectron lines depicts the exit of the photoelectron from the metal surface. The time elapsed between the creation of a photoelectron and its exit from the surface is τ . This implies that the photoelectron does not interact with the metal beyond this time; i.e., no interaction lines are to be attached to the photoelectron line above the black dot.

In the RPA the effective interaction (represented by the line of chain) is given as

$$\mathcal{V}(q, \omega) = v(q) / \epsilon(q, \omega), \quad (1)$$

where $v(q) = 4\pi e^2 / q^2$ is the bare Coulomb interaction and $\epsilon(q, \omega)$ is the Lindhard dielectric function. We separate the potential into two terms as

$$\mathcal{V}(q, \omega) = V(q, \omega) + U(q, \omega). \quad (2)$$

The first term $V(q, \omega)$ takes into account the short-range part of the effective Coulomb interaction as shown in Fig. 2 and we call such a term the single-pair term. The contribution of this term can be written as

$$V(q, \omega) = v_s(q) + [v_s(q)]^2 [-B(q, \omega)], \quad (3)$$

where $v_s(q)$ is the screened Coulomb potential

$$v_s(q) = v(q) / \epsilon(q, 0) \quad (4)$$

and $-B(q, \omega)$ is the contribution of the bubble diagram corresponding to the single particle-hole pair creation. It is related to the RPA dielectric function as

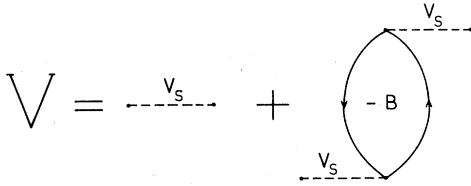


FIG. 2. Short-range part of the effective Coulomb interaction which includes the statically screened Coulomb interaction and the dynamic contribution due to single-pair production ($-B$).

$$\epsilon(q, \omega) = 1 + v(q)B(q, \omega). \quad (5)$$

The second term $U(q, \omega)$ of Eq. (2) can then be obtained from the difference

$$U(q, \omega) = \mathcal{V}(q, \omega) - V(q, \omega) \quad (6)$$

where $\mathcal{V}(q, \omega)$ and $V(q, \omega)$ are given by Eqs. (1) and (3), respectively.

In the next section we consider the many-body interaction effects due to the single-pair potential $V(q, \omega)$, which are known to introduce the infrared catastrophe already studied in a simplified model by DS. In Sec. IV we consider the many-body effects related to the complete dynamical potential $\mathcal{V}(q, \omega)$ of Eq. (2). This term accounts for the occurrence of the plasmon satellites and the low-energy background intensity. In Sec. V we present the results of our theory for Na and Al with special attention to the ultrasoft XPS.

III. LOW-ENERGY PAIR PRODUCTION

The effect of low-energy electron-hole pair creation on the x-ray emission and absorption spectra of metals was first treated by Nozières and deDominicis (ND).¹⁴ Such excitations were found to be responsible for the anomalous behavior at the emission and absorption edge. This theory was then applied to the XPS by DS.² By a direct application of the ND theory, these authors showed that the XPS intensity is also given by a power law and the result could be expressed as

$$I^s(\epsilon) = \frac{1}{\pi} \operatorname{Re} \int_0^\infty ds y(s) e^{i(\epsilon + i\lambda)s}, \quad (7)$$

with $y(s) = (i\xi_0 s)^{-\alpha}$ and $\epsilon \equiv \omega + \epsilon_B - \epsilon_k$ (see notations of Fig. 1). The width λ is related to the damping of the final states and is treated in detail below. The factor $e^{-\lambda s}$ appears in Eq. (7), essentially because the photoelectron final states are not relaxed. Indeed, the photoelectron is detected before being completely damped. This does not occur in the XPA, where the golden rule includes *all* final states. Exponent α is a function of the phase shift of the conduction electrons at the Fer-

mi level, due to scattering by the core-hole potential, and can be related to the phase shifts by

$$\alpha = 2 \sum_{l=0}^{\infty} (2l+1) \left(\frac{\delta_l}{\pi} \right)^2. \quad (8)$$

Note that it differs from the ND exponent in the XPA by the absence of a term $-2\delta_l/\pi$ which is related to the replacement effect. In the XPS, the photoelectron energy is quite different from the Fermi energy and hence no infrared catastrophe due to *weak* pair-replacement effect can occur. The role of the replacement term in the simplified DS model for the photoemission is simply to multiply $I^s(\epsilon)$ by a constant vertex correction term and it is thus disregarded. In our detailed theory this term is no longer constant. However, since its behavior is nonsingular at $\epsilon \approx 0$, we postpone its discussion until Sec. IV.

If, in Eq. (7), the width λ is taken to be zero, one has

$$I^s(\epsilon) = \frac{\Gamma(1-\alpha)}{\pi \xi_0} \left(\frac{\xi_0}{\epsilon} \right)^{1-\alpha} \Theta(\epsilon) \sin \pi \alpha, \quad (9)$$

where Θ is the step function. This expression thus replaces the line shape $I^s(\epsilon) = \delta(\epsilon)$ which would be obtained in a one-body calculation. Note that $I^s(\epsilon)$ given by Eq. (9) is nonintegrable for large values of ϵ (this is true even for a nonvanishing λ). This is due to the simplifications involved in the DS model which is valid only for $\epsilon \ll \epsilon_F$. For a realistic model, however, $I^s(\epsilon)$ must be integrable for all ϵ . This also emphasizes that the DS theory must be modified in order that it may be valid at lower photoelectron energies (large ϵ). Such an expansion of the DS theory requires an ϵ dependence of α , ξ_0 , and λ , which have so far been considered to be constants.

To extend the DS theory beyond the close neighborhood of $\epsilon \sim 0$, i.e., to determine the functions $\alpha(\epsilon)$ and $\xi_0(\epsilon)$, we will proceed in the following way. When the integration in Eq. (7) is carried out one obtains

$$I^s(\epsilon) = \frac{\Gamma(1-\alpha)}{\pi \xi_0^2 (\epsilon^2 + \lambda^2)^{(1-\alpha)/2}} \times \cos \left[\frac{\pi \alpha}{2} - (1-\alpha) \tan^{-1} \left(\frac{\epsilon}{\lambda} \right) \right], \quad (10)$$

which is then expanded up to first order in α and λ to find

$$I^s(\epsilon) \approx \delta(\epsilon) + \alpha \left(\delta(\epsilon) \ln \frac{|\epsilon|}{e^{-\gamma} \xi_0} - \frac{P}{\epsilon} \Theta(\epsilon) \right) - \frac{\lambda}{\pi} \frac{d}{d\epsilon} \left(\frac{P}{\epsilon} \right) \quad (11)$$

($\gamma = 0.577$ is the Euler constant).

Let us now carry out a calculation up to first order in simple pair interaction $V(q, \omega)$. Such a

lowest-order calculation can be performed completely and will yield an expression of $I^s(\epsilon)$ which can be formally identified with Eq. (11) giving ϵ -dependent expressions for α , ξ , and λ . Such expressions, linear in $V(q, \omega)$, are not singular for $\epsilon \rightarrow 0$ and can be considered to be quite satisfactory for all values of ϵ . When these functions are calculated, they can be substituted for the constants α , ξ , and λ in Eq. (10). This gives an expression of $I^s(\epsilon)$ which has a power-law character for small ϵ and is also physically correct for large ϵ , since for large ϵ the first-order calculation is known to give good results. Before proceeding to more explicit evaluation of these functions we would like to make some comments.

In their theories Nozières and deDominicis,¹⁴ and Doniach and Šunjić² (ND-DS) neglect the effect of particle-hole pair creation due to scattering by the electrons (or holes) in the conduction band. ND-DS are mainly concerned with the effect of particle-hole creation due to scattering by the core hole via a static screened Coulomb interaction. They include the multiple scattering effects by summing ladder diagrams (K matrix). In this paper however, we are interested in incorporating all possible many-body effects in terms of the RPA effective interaction $\mathcal{U}(q, \omega)$ given by Eq. (2) (see Sec. IV). The interactions considered by ND-DS are essentially contained in the single-pair part $V(q, \omega)$ given by Eq. (3) and represented in Fig. 2. Referring to Fig. 3, which depicts the basic photoemission process along with various single-pair processes, we have to point out that RPA calculation does not describe multiple-vertex loops and open lines, e.g., elements a and b , but includes only two vertex loops like c and one-vertex open lines like d . In other words, our ap-

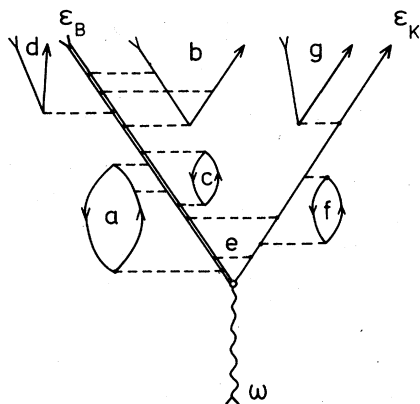


FIG. 3. Diagrammatic representation of the basic photoemission process along with various single-pair excitations.

proach consists of replacing the K matrix used by ND-DS (ladder diagrams) by the screened Coulomb interaction given by Eq. (4).

This approach is justified, however, and at the end of this section we will show that this is equivalent to calculating the phase shifts δ_l 's appearing in the exponent α [Eq. (8)] in the Born approximation. Such a first-order calculation of the phase shifts in the Born approximation has been found to be quite satisfactory.¹⁵ These phase shifts satisfy the Friedel sum rule, and the difference between these and the actual phase shifts is never more than 10%. We must also point out that, unlike the case of the replacement term of the x-ray band spectra, the scatterings corresponding to large q values do not play any essential role in the photoelectron spectra.¹⁶ Thus the pseudopotential corrections for large q values (short-range correction) can be neglected and the structureless potential given by Eq. (4) can be used for all values of q (or equivalently one can use plane waves instead of Bloch waves for the conduction states). These points are discussed in greater detail towards the end of this section.

Our next comment is regarding the neglect of the conduction-electron interaction effects by ND-DS. These authors have neglected contributions from the open particle-hole lines and the closed self-energy parts, such as the elements f and g of Fig. 3. However, in the present general theory we must include the contributions from these diagrams. Note that the self-energy part f is responsible for the finite lifetime of the photoelectron, which in turn gives rise to the width λ appearing in Eq. (7) and in the last singular term of Eq. (11). In DS such a width is introduced as a parameter to obtain a realistic line shape and is related to the core-hole lifetime. However, the width of the core hole, in general, is much weaker than the width of the photoelectron occurring due to single particle or plasmon excitations. In fact, the width λ is related to the imaginary part of the self-energies of the electrons and the holes of the final state. Let us write $\lambda = \lambda_h + \lambda_e$, where λ_h is the core-hole width and λ_e , the photoelectron width. In the RPA, one has

$$\lambda_h = -\frac{1}{(2\pi)^3} \int d\vec{q} \operatorname{Im} \mathcal{U}_+(q, 0) = 0,$$

and the width of the photoelectron

$$\lambda = \lambda_e = -\frac{1}{(2\pi)^3} \int d\vec{q} \operatorname{Im} \mathcal{U}_+(q, \epsilon_h - \epsilon_{\vec{k}-\vec{q}}). \quad (12)$$

The core-hole damping is strictly zero as long as we do not consider its Auger width, which is also negligible in comparison with λ_e . Thus, it is quite reasonable and consistent that in our model

we relate λ essentially to the photoelectron damping and not to either the core-hole damping or to some undefined instrumental width.

We now proceed to the main point of this section which is the explicit evaluation of the function $\alpha(\epsilon)$ and $\xi_0(\epsilon)$. The correlation function $y(s)e^{-i(\epsilon_k - \epsilon)s}$ appearing in the integrand of Eq. (7) can, in a first-order calculation, be related to the four diagrams of Fig. 4.

As indicated before, we consider contributions of only those parts of these diagrams which correspond to the *singular* terms of Eq. (11). The total contribution of the zeroth order diagram 0 is given by the first term of Eq. (11). Diagram A will have two parts corresponding to the two terms of $V(q, \omega)$ given in Eq. (2). In this section we consider the contribution from the first term $V(q, \omega)$ since, as mentioned before, this is the term leading to the singularity of the second term of Eq. (11). The contribution of the second term $U(q, \omega)$ of Eq. (2) is nonsingular and will be treated in the next section. Diagrams B and C do not introduce any singularity and hence we consider them in the next section. Note that in the XPA diagram B would be related to the replacement effect.

The correlation function can now be calculated by using diagrammatic rules. One obtains

$$y(s) = 1 + \frac{i}{(2\pi)^4} \int d\vec{q} \int d\omega' \frac{e^{-i\omega's} - 1}{\omega'(\omega' - i\delta)} V(q, \omega), \quad (13)$$

where the first and second terms correspond to contributions from diagrams 0 and A, respectively (δ is an infinitesimal constant). The intensity $I^s(\epsilon)$, given by Eq. (7), can then be calculated up to the first order in λ using the relation

$$\left(\frac{\partial}{\partial \omega} \text{Re} V_+(q, \omega) \right)_{\omega=0} = \frac{1}{\pi} \int_0^\infty \frac{d\omega'}{\omega'^2} \text{Im} V_+(q, \omega').$$

One obtains

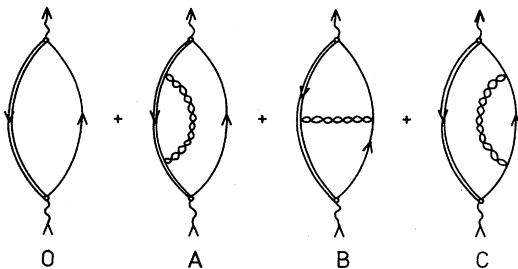


FIG. 4. Diagrams in zero and first order in effective Coulomb interaction contributing to the x-ray photoemission spectra of metals.

$$I^s(\epsilon) = \delta(\epsilon) - \int_0^\infty d\omega' \alpha(\omega') \left(\text{P} \frac{\delta(\epsilon)}{\omega' - \epsilon} - \frac{\delta(\omega' - \epsilon)}{\epsilon} \right) - \frac{\lambda}{\pi} \frac{d}{d\epsilon} \left(\frac{\text{P}}{\epsilon} \right), \quad (14)$$

with

$$\alpha(\omega') \equiv - \frac{1}{\pi(2\pi)^3 \omega'} \int d\vec{q} \text{Im} V_+(q, \omega'),$$

where the subscript + means that part of the V function which is analytic in the upper half of the complex ω plane ($\text{Im}\omega > 0$). Equation (14) will have the same form as Eq. (11), if we let

$$\text{P} \int d\omega' \frac{\alpha(\omega')}{\omega' - \epsilon} \equiv \alpha(\epsilon) \ln \frac{e^{-\gamma} \xi_0(\epsilon)}{|\epsilon|}. \quad (15)$$

But now α and ξ_0 are no longer constants but are ϵ -dependent functions given by

$$\alpha(\epsilon) = \frac{1}{\pi(2\pi)^3 \epsilon} \int d\vec{q} [v_s(q)]^2 \text{Im} B_+(q, \epsilon) \quad (16)$$

and

$$\xi_0(\epsilon) = |\epsilon| \exp \left(\gamma + \frac{1}{\alpha(\epsilon)} \text{P} \int d\omega' \frac{\alpha(\omega')}{\omega' - \epsilon} \right). \quad (17)$$

These functions and λ given by Eq. (12) can finally be substituted in Eq. (10) to obtain the XPS intensity. The procedure of this section thus enables us to extend the DS calculations to lower energies by using a realistic core-hole potential.

Before proceeding to the next section, where we consider the effect of extrinsic losses on XPS, let us demonstrate that $\alpha(0)$ does correspond to the DS exponent [Eq. (8)] where δ_i 's are the Born phase shifts. For small frequencies, $\text{Im} B_+(q, \epsilon) = \text{Im} \epsilon(q, \epsilon)/v(q)$ has the form

$$\text{Im} B_+(q, \epsilon \sim 0) \approx \frac{m^2 \epsilon}{2\pi q} \Theta(2k_F - q).$$

Hence from Eq. (16)

$$\alpha(0) = \frac{m^2}{4\pi^4} \int_0^{2k_F} dq q [v_s(q)]^2.$$

Using the Born expression for the phase shifts

$$\delta_i = \frac{m}{4\pi k_F} \int_0^{2k_F} dq q v_s(q) P_i \left(1 - \frac{q^2}{2k_F^2} \right),$$

it can be shown¹⁵ that

$$\alpha(0) = 2 \sum (2l+1) \left(\frac{\delta_l}{\pi} \right)^2.$$

IV. BACKGROUND AND PLASMON PRODUCTION

As we have alluded to before, there are two types of energy losses (due to electron-hole pair creation and plasmon production) in the photoemission process: the intrinsic losses which can

be considered as an integral part of the photoproduction process, and the extrinsic losses which correspond to the loss of energy by a photoelectron during its flight to the metal surface. Moreover, there is a quantum interference between these intrinsic and extrinsic processes, which produces a cancellation effect that becomes particularly important when the initial photoelectron energy $\epsilon_k = \omega + \epsilon_B$ is weak (of the order of a few ω_p 's).

In Sec. III, the calculation of the intrinsic loss has been carried out by the method of linear response only for the V part of the effective interaction $\mathcal{V}(q, \omega)$ [see Eq. (7)]. This method is suited to calculate the effect of low-energy pair production during the XPS process. A broadening effect due to the nonrelaxed nature of the photoelectron state has also been introduced in Eq. (7) as an "external correction." Thus, the linear response formalism of Sec. III has incorporated only those extrinsic processes which are due to the final state width. Such a formulation cannot calculate the change in the intensity and the shape, due to extrinsic processes. In other words, it cannot calculate the extrinsic part of the plasmon satellite and the continuum. Indeed, these extrinsic excitations depend on the depth z at which the photoelectron is created (or the time $\tau = -z/V_k$ taken by the photoelectron to reach the surface). This fact plays an essential role in the calculation of both the extrinsic processes and the quantum interference term.

Calculation of the extrinsic energy losses and their quantum interference with the intrinsic ones presents real difficulties since it should, in principle, include multiple convolutions between successive excitations along the path z . However, in this paper we are mainly interested in that part of the continuum and satellite production which mostly depends on the initial energy of the photoelectron $\epsilon_k = \omega + \epsilon_B$. Thus, the most relevant extrinsic loss to consider is the *first* loss which occurs right after the phototransition process. It is also this loss (pair or plasmon production) which will be most affected by the interference with the intrinsic loss and thus will strongly de-

pend on $\omega + \epsilon_B$. We thus consider the spectral region covering the main line and the first satellite, where the effect of the quantum interference term on the first-order extrinsic process is particularly important.

Let us consider a semi-infinite metal occupying the region $z \leq 0$. Let $J(z, \epsilon_k)$ be the intensity of the photoelectron produced in a shell of unit thickness at a depth z and leaving the metal (at $z=0$) with an energy ϵ_k . For simplicity we assume that the photoelectron path is normal to the surface and its energy is large enough (at least a few ω_p 's), such that the motion across the metal is quasistraight and uniform. Under these conditions the observed intensity is given by

$$I(\epsilon_k) = \int_{-\infty}^0 dz \rho(z) J(z, \epsilon_k), \quad (18)$$

where $\rho(z)$ is the density of the core holes, which in our calculation is assumed to be constant and equal to one.

We first consider a model in which the excitation produced by a photoelectron has only one possible energy. Writing the effective potential in the form

$$\begin{aligned} \mathcal{V}_+(q, \omega) &= -\frac{1}{\pi} \int_0^\infty d\omega' \frac{\text{Im}\mathcal{V}_+(q, \omega')}{\omega - \omega' + i\lambda} \\ &= \sum_{\omega'} \frac{c(q, \omega')}{\omega - \omega' + i\lambda}, \end{aligned} \quad (19)$$

we see that each term in this "sum" is related to such an excitation and that

$$c(q, \omega') = -(1/\pi)\Delta\omega' \text{Im}\mathcal{V}_+(q, \omega')$$

is the square of the electronic coupling constant. As an example of such a model consider the excitation of an undamped dispersionless plasmon where

$$c(q, \omega_p) = \frac{1}{2}\omega_p v(q) \quad \text{for } q < q_c.$$

Ignoring the internal interaction lines of Fig. 1, we find that the S -matrix element related to photoemission accompanied by n excitations (n external interaction lines) has the form

$$S_n(\tau, \epsilon_k) = \frac{1}{i} \int dt g(t) e^{i(\epsilon_k + n\omega' - \epsilon_B - \omega)t} \frac{1}{n!} \prod_{\mu=1}^n \left[\frac{1}{i} \left(\frac{c(q_\mu, \omega')}{(2\pi)^3} \right)^{1/2} \left(\frac{1}{\omega'} - \frac{1 - \exp(i\nu_\mu \tau)}{\nu_\mu} \right) \right], \quad (20)$$

with

$$\nu_\mu = \omega' + \epsilon_k - \epsilon_{|\vec{k} + \vec{q}_\mu|} = \omega' + (2\vec{k} \cdot \vec{q}_\mu - q_\mu^2)/2m$$

and

$$S_0(\tau, \epsilon_k) = \frac{1}{i} \int dt g(t) e^{i(\epsilon_k - \epsilon_B - \omega)t},$$

where t is the time at which the photoelectron is produced and $t + \tau$ is the time of its exit from the metal. Function $g(t)$ is the adiabatic function

$$\begin{aligned} g(t) &= 1 \quad \text{for } |t| \leq t_0/2 \\ &= 0 \quad \text{for } |t| \geq t_0/2, \end{aligned}$$

with $t_0 \gg \tau$ and such that

$$\left| \int dt g(t) e^{i\nu t} \right|^2 \cdots = 2\pi t_0 \delta(\nu) \cdots$$

Expression (20) contains an approximation which was first used by Chastenet and Longe in a recent paper.¹⁷ Propagators $1/\omega'$ and $1/\nu_\mu$ are related to the core hole and the internal photoelectron lines, respectively. In calculating the photoelectron propagator, they make the assumption that the photoelectron energy $\omega + \epsilon_B$ remains unchanged across the excitation vertices even though the momentum is conserved at all vertices. For the core hole, however, the fact that ϵ_B remains constant across the intrinsic vertices is physically exact since it is recoilless. Thus a property of the core-hole propagators is attributed to the photoelectron propagators. This approximation is better than in the previous papers. Indeed, for virtual states the requirement of energy conservation is not as crucial as the requirement of momentum conservation which must be satisfied, especially for small k 's.

It is easy to show, however, that the main line ($n=0$) and the first plasmon satellite loss ($n=1$) are not affected at all by this approximation, although it will slightly affect the spectrum for $n \geq 2$. The approximation of using $1/\nu_\mu$ for the internal photoelectron propagator introduces a relative error in Eq. (20) given by

$$\frac{\Delta S_n}{S_n} \approx \sum_{\mu=1}^n \frac{\Delta \nu_\mu}{\nu_\mu},$$

with $\Delta \nu_\mu \approx \Delta k q_\mu / m < \Delta k q_c / m$ and $\nu_\mu \approx \omega'$. Since the error in the energy transferred by the μ th internal line is $\Delta \epsilon_k = k \Delta k / m = (\mu - 1)\omega'$, one has $\Delta \nu_\mu / \nu_\mu < (\mu - 1)q_c / k$; hence $\Delta S_n / S_n < n(n - 1)q_c / 2k$. Thus Eq. (20) is exact for $n=0$ and $n=1$ and for higher-order losses it can be considered that the approximated energy transfer will give excellent results even for small k 's. We conclude from this discussion that even though the photoemission intensity in the main line and the first plasmon satellite regions is governed by all such higher-order losses, the effect of the above approximations on these intensities will be small.

The photoelectron intensity with n excitations is then given by the τ -dependent golden rule

$$J_n(\tau, \epsilon_k) = \frac{1}{2\pi N t_0} \sum_f |S_n(\tau, \epsilon_k)|^2, \quad (21)$$

where N is a normalization constant. The summation over the final states

$$\sum_f \cdots = n! \int dq_1 \cdots \int dq_n \cdots \quad (22)$$

gives

$$J_n(\tau, \epsilon_k) = \delta(\epsilon_k + n\omega' - \epsilon_B - \omega) (Nn!)^{-1} [T(\tau, \epsilon_k)]^n, \quad (23)$$

where $T(\tau, \epsilon_k)$ is a T -matrix element given by

$$T(\tau, \epsilon_k) = \frac{1}{(2\pi)^3} \int d\vec{q} c(q, \omega') \left| \frac{1}{\omega'} - \frac{1 - \exp(i\nu_q \tau)}{\nu_q} \right|^2. \quad (24)$$

For $\tau\omega_p \gg 1$, a condition always satisfied (except for ultrathin films), $T(\tau, \epsilon_k)$ takes the form

$$T(\tau, \epsilon_k) = \beta - f(\epsilon_k) + \Gamma(\epsilon_k)\tau, \quad (25)$$

with

$$\beta \equiv \frac{1}{(2\pi)^3 \omega'^2} \int d\vec{q} c(q, \omega'), \quad (26a)$$

$$f(\epsilon_k) \equiv \frac{2}{(2\pi)^3 \omega'} P \int d\vec{q} \frac{c(q, \omega')}{\nu_q}, \quad (26b)$$

$$\Gamma(\epsilon_k) \equiv \frac{1}{(2\pi)^2} \int d\vec{q} c(q, \omega') \delta(\nu_q), \quad (26c)$$

which correspond to the intrinsic, the interference, and the extrinsic terms, respectively. The intrinsic term (26a) and the extrinsic term (26c) are in the forms, respectively, suggested by Lundqvist¹ and by Chang and Langreth⁴ for the dispersionless plasmon. However, these latter authors have calculated the interference term only in a lowest-order expansion. As already mentioned the calculation in the present paper is exact at least for $n=0$ and 1.

Finally, the normalization constant N in Eq. (23) is calculated by using a sum rule

$$\int_{\epsilon_F}^{\omega + \epsilon_B} d\epsilon_k \sum_n J_n(\tau, \epsilon_k) = 1, \quad (27)$$

which is required by the conservation of the number of photoelectrons. For practical reasons, we evaluate N approximately by making it ϵ_k dependent and writing

$$N = \exp T^*(\tau, \epsilon_k), \quad (28)$$

with $T^* = \beta - f^* + \Gamma^* \tau$. The starred functions are obtained from the unstarred ones given by Eqs. (26b) and (26c), by replacing \vec{k} and $\vec{k} + \vec{q}$ by $\vec{k} - \vec{q}$ and \vec{k} , respectively. This means that the starred expressions are related to the decay of an electron from a state \vec{k} to a state $\vec{k} - \vec{q}$, whereas the corresponding unstarred quantities are related to the creation of an electron in state \vec{k} from a state $\vec{k} + \vec{q}$. In both cases an excitation of momentum \vec{q} is produced. Expression (28) for N can be interpreted as follows. First it satisfies the conservation requirement (27). Moreover, the extrinsic production (τ -dependent part of J_n) takes the form $(\Gamma_n \tau)^n e^{-\Gamma_n^* \tau} / n!$, which is an approximate solution for the classical Poisson equation $dJ_n/d\tau$

$= \Gamma_n J_{n-1} - \Gamma_n^* J_n$, where Γ_n and Γ_n^* depend on n , i. e., on ϵ_k , the exact solutions of this set of Poisson's equations satisfying the sum rule (27). The total photoemission intensity from a uniformly ionized semi-infinite metal can then be calculated using Eq. (18). One obtains

$$I_n(\epsilon_k) = \int_0^\infty d\tau V_k J_n(\tau, \epsilon_k) \\ = \delta(\epsilon_k + n\omega' - \epsilon_B - \omega) \frac{V_k}{\Gamma_n^*(\epsilon_k)} e^{-\beta'(\epsilon_k)} \\ \times \sum_{\mu=0}^n \frac{[\beta'(\epsilon_k)]^\mu}{\mu!} \left(\frac{\Gamma(\epsilon_k)}{\Gamma_n^*(\epsilon_k)} \right)^{n-\mu}, \quad (29)$$

with $\beta'(\epsilon_k) \equiv \beta - f(\epsilon_k)$.

For the main line ($n=0$) and the first satellite line ($n=1$), expression (29) becomes

$$I_0(\epsilon_k) = \delta(\epsilon_k - \epsilon_B - \omega) [V_k / \Gamma^*(\epsilon_k)] e^{-\beta'(\epsilon_k)} \quad (30)$$

and

$$I_1(\epsilon_k) = \delta(\epsilon_k + \omega' - \epsilon_B - \omega) \frac{V_k}{\Gamma^*(\epsilon_k)} \\ \times \left(\beta - f(\epsilon_k) + \frac{\Gamma(\epsilon_k)}{\Gamma^*(\epsilon_k)} \right) e^{-\beta'(\epsilon_k)}. \quad (31)$$

The last step consists in investigating the realistic model where all excitations appearing in Eq. (19) are considered. In such a case, Eqs. (20), (22), (23), (24), and (28) are respectively replaced by the following extended forms:

$$S_n(\tau, \epsilon_k) = \frac{1}{i} \int dt g(t) e^{i(\epsilon_k - \epsilon_B - \omega)t} \frac{1}{n!} \prod_{\mu=1}^n \left[\frac{1}{i} \left(\frac{c(q_\mu, \omega'_\mu)}{(2\pi)^3} \right)^{1/2} e^{i\omega'_\mu t} \left(\frac{1}{\omega'_\mu} - \frac{1 - \exp(i\nu_\mu \tau)}{\nu_\mu} \right) \right], \quad (20')$$

$$\sum_f \dots = n! \sum_{\omega'_1} \int dq_1 \dots \sum_{\omega'_n} \int dq_n \dots, \quad (22')$$

$$J_n(\tau, \epsilon_k) = (Nn!)^{-1} \left(\prod_{\mu=1}^n \int d\omega'_\mu T(\tau, \epsilon_k, \omega'_\mu) \right) \bar{\delta} \left(\epsilon_k - \epsilon_B - \omega - \sum_{\mu=1}^n \omega'_\mu \right), \quad (23')$$

i. e.,

$$J_0 = N^{-1} \bar{\delta}(\epsilon_k - \epsilon_B - \omega), \quad (23a')$$

$$J_1 = N^{-1} \int d\omega' T(\tau, \epsilon_k, \omega') \bar{\delta}(\epsilon_k - \epsilon_B - \omega - \omega'), \quad (23b')$$

$$T(\tau, \epsilon_k, \omega') = \frac{-1}{\pi(2\pi)^3} \int d\vec{q} \left(\text{Im} \mathcal{V}_+(q, \omega') \left| \frac{1}{\omega'} - \frac{1 - \exp(i\nu_{\vec{q}} \tau)}{\nu_{\vec{q}}} \right|^2 - \text{Im} V_+(q, \omega') \frac{1}{\omega'^2} \right), \quad (24')$$

and

$$N = \exp \int d\omega' T^*(\tau, \epsilon_k, \omega'). \quad (28')$$

An important comment regarding the connection between the calculation of the present section with that of the preceding section is in order. In Sec. III we have evaluated the contribution of the V part of the effective interaction in the linear approximation and have found that it gives rise to the infrared catastrophe. The shape of the main line differs from the zeroth-order shape (δ function) over a small energy range (a small fraction of the Fermi energy). The calculations of both sections are now combined in a unified theory by including the function I^s of Sec. III into the $\bar{\delta}$ functions of Eqs. (23a') and (23b'). These $\bar{\delta}$ functions can then be considered as quasi- δ functions.

However, to avoid duplication of use of the V part of the potential \mathcal{V} , we must subtract the V part from the intrinsic contribution in the T (or T^*) function. This is precisely the reason for introducing the second term ($-\text{Im} V_+ / \omega'^2$) in Eq.

(24'). This theory is thus consistent in that the ND-DS structure of the main line has been retained and that function T is not singular for $\omega' \sim 0$, as it would have been if the second term in Eq. (24') were missing. Function T thus describes the excitation of the first satellite and that part of the continuum which occurs due to a single excitation of the particle-hole pair. This function appears as the sum of the following contributions: the intrinsic contribution

$$\beta(\epsilon_k, \omega') = -\frac{1}{\pi(2\pi)^3} \frac{1}{\omega'^2} \int d\vec{q} \text{Im} [\mathcal{V}(q, \omega') - V(q, \omega')], \quad (26a')$$

the extrinsic contribution

$$\Gamma(\epsilon_k, \omega') \tau = -\frac{\tau}{\pi(2\pi)^3} \int d\vec{q} \text{Im} \mathcal{V}(q, \omega') \delta(\omega' + \epsilon_k - \epsilon_{\vec{k} + \vec{q}}), \quad (26c')$$

which is τ dependent and is written for $\omega_p \tau \gg 1$; and finally the negative interference contribution

$$f(\epsilon_k, \omega') = \frac{2}{\pi(2\pi)^3 \omega'} P \int d\vec{q} \frac{\text{Im} \mathcal{V}_+(q, \omega')}{\omega' + \epsilon_k - \epsilon_{\vec{k} + \vec{q}}}. \quad (26b')$$

It is interesting to note that for $\tau \rightarrow \infty$, the first term of Eq. (24') becomes similar to the basic expression describing the x-ray spectra

$$T_x(\epsilon_k, \omega') = -\frac{1}{\pi(2\pi)^3} \int d\vec{q} \text{Im} \mathcal{V}_+(q, \omega') \left| \frac{1}{\omega'} - \frac{1}{\nu_q} \right|^2,$$

which is valid as long as ν_q 's do not vanish. This emphasizes the fact that our calculation is valid up to the ultrasoft-x-ray regime.

Let us finally give the expressions for the total photoemission intensity from a semi-infinite metal. Using Eq. (29), and expression (28') for N , one obtains

$$I_0(\epsilon_k) = I^s(-\epsilon_k + \epsilon_B + \omega) V_k \frac{\exp[-\int d\omega' \beta'^*(\epsilon_k, \omega')]}{\int d\omega' \Gamma^*(\epsilon_k, \omega')} \quad (30')$$

and

$$I_1(\epsilon_k) = V_k \frac{\exp[-\int d\omega' \beta'^*(\epsilon_k, \omega')]}{\int d\omega' \Gamma^*(\epsilon_k, \omega')} \times \int d\omega'' I^s(-\epsilon_k + \omega'' + \epsilon_B + \omega) \times \left(\beta'(\epsilon_k, \omega'') + \frac{\Gamma(\epsilon_k, \omega'')}{\int d\omega' \Gamma^*(\epsilon_k, \omega')} \right). \quad (31')$$

V. DISCUSSION AND RESULTS

Before we present our results, let us reiterate some of the salient features of our theory and its connection with previous theories. Our theory has been termed *unified* in the sense that it describes the XPS intensity over the spectral range, including the first plasmon satellite and the main band. The validity of the theory is exemplified by the fact that it is in "asymptotic" agreement with three previous theories which have successfully described the spectral structures in different spectral regions in various electron and x-ray spectroscopies. Let us recall that these three theories are

(a) the theory of soft-x-ray spectra^{18,16,12} (emission and absorption) using a first-order expansion of the RPA effective potential,

(b) the theory of edge effect^{14,2} (x-ray emission and absorption, photoemission, and Auger emission) using an all-order expansion with a separable static potential (ND-DS theory), and

(c) the theory of plasmon production in high-energy photoemission,^{1,4,5} using electron-plasmon interaction effects to all orders.

Let us make some comments on the validity and limitations of these theories and their relationship with our work. The linear theory (a) is,

in principle, valid in the entire spectral region of the x-ray spectra. It is particularly suited to describe the cancellation effects between the intrinsic and extrinsic effects, which become important when the energies involved are of the order of Fermi energy or the plasmon energy (weak energies). Consequently, this theory describes the low-energy features¹⁸ (tailing and the plasmon satellites) with excellent agreement with the observed spectra. However, this theory partially fails to describe the edge effect¹⁶ which appears as an infrared catastrophe that cannot be described by a linear theory. Indeed, in this linear theory the power law $(\xi_0/\epsilon)^{-\alpha}$ describing the edge effect becomes linear in the interaction potential and logarithmic in the energy, i.e., $1 - \alpha \ln(\xi_0/\epsilon)$. It is interesting to note, however, that the coefficient α of $\ln \epsilon$ is in agreement with the exponent of the edge theory (b), but it is expressed as a function of the phase shift δ_l 's calculated by the Born linear approximation.¹⁵ However, the Born phase shifts are in approximate agreement with the phase shifts calculated by means of more elaborate methods.¹⁹ Such an agreement is not surprising since the Born phase shifts also satisfy the Friedel sum rule, the form of which is not modified by the linearization. Furthermore, δ_l 's for $l \geq 1$ are calculated with satisfactory accuracy in the Born approximation (at most 10% error for δ_1) since only the peripheral of the potential is involved in such calculations. The same accuracy can also be attributed to the Born δ_0 , because of the validity of the Friedel sum rule. It appears as if the small error in the Born approximation due to linear use of the long-range part of the potential ($l \geq 1$) is exactly compensated by the error due to the simplified treatment of the short-range structure. Such a compensation is normal in view of the physical significance of the Friedel sum rule. The linear theory thus gives valuable results not only for the low-energy structures of the spectra but also regarding the exponent of the ND-DS power law. This theory also shows that the short-range structure of the potential, in general, plays a negligible role¹⁶ (i.e., the core hole can be treated as a point charge) except in one term. This is the term that describes the replacement effect related to the factor $-2\delta_l/\pi$ of the ND exponent (for the theory of x-ray spectra) for which larger momentum transfers play an important role.¹⁶ However, as we have discussed in Sec. III, in XPS this effect does not occur at all as the photoelectron energy is too high compared with the Fermi energy to give rise to weak pair replacements. This justifies the use of the dynamically screened Coulomb potential to describe the core-hole interaction in XPS studies.

The validity of theory (b) is limited in the frequency regions presenting spectral discontinuities (x-ray edge frequency, photoemission line frequency), where the cumulative effect of the weak pair creations becomes important. However, this theory neglects the realistic form and the dynamical nature of the core-hole potential as it uses a separable potential instead. The inelastic scatterings of electrons and holes (self-energies) are also neglected. The ND-DS theory thus gives nothing more than the correct expression for the exponent of the power law. However, this gives us a sufficient clue to introduce nonlinear corrections in theory (a), which make it consistent with theory (b) in the regions of spectral discontinuities. Thus our theory gives good results in the low-energy regions where the cancellation effects are important, as well as in the main line region which shows the spectral discontinuity.

Theory (c) deals with the problem of multiple plasmon productions (satellite series) during photoemission for high incident photon energies. In general, the photoelectron is treated semiclassically as an external potential.^{4,5} The most complete treatment of the multiple plasmon production is due to Langreth *et al.*⁴ They give the rates of intrinsic and extrinsic plasmon productions and the effect of their interference, for the case of high energy of the incident photons. Chastenet and Longe¹⁷ have extended this theory to include all incident photon energies and have shown that it is in agreement with theory (a) for low energies. The calculation of the latter authors, which bridges theories (a) and (c), has been extended in the present paper by including not only the effect of plasmon production but also that of the single-pair creation. Unlike the previous authors, we have also included the effect of dispersion and attenuation of the plasmon in our calculation.

The intensity and the shape of the photoemission spectra in the main line and the plasmon satellite regions can be obtained when one considers Eq. (10) of Sec. III together with Eqs. (12), (16), and (17), as well as Eqs. (30') and (31') of the preceding section.

We have carried out numerical computations for Na ($r_s = 3.993$) and for Al ($r_s = 2.0737$) for two values of the incident photon energies $\omega + \epsilon_B = 5\omega_p$ and $90\omega_p$. For Na ($\omega_p = 5.91$ eV) these energy values correspond to 29.5 eV and 531 eV, and for Al ($\omega_p = 15.8$ eV) these correspond to 78.9 and 1420 eV, respectively. Let us emphasize that the excitation energies and the electron density parameter r_s are the only two parameters appearing in our calculation and as such it can be considered to be an *ab initio* calculation. The results of our calculation are shown in Figs. 5 and 6. In these

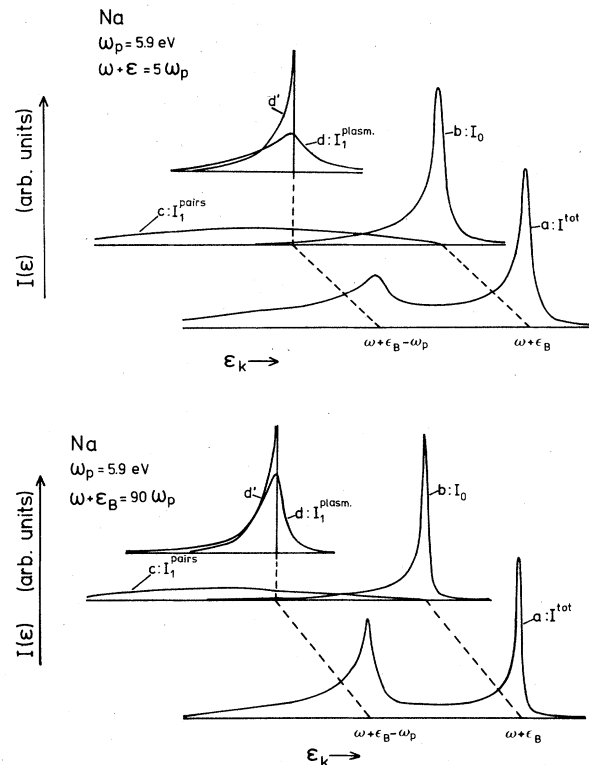


FIG. 5. (a) x-ray photoemission intensity in the main line and the first plasmon satellite region in Na at the excitation energy of $5\omega_p$ (29.5 eV). The total intensity is given by curve *a*. Curves *b*, *c*, and *d* are the main line, the background due to single-pair excitation, and the satellite due to one-plasmon production, respectively. (b) x-ray photoemission intensity of Na for the incident photon energy of $90\omega_p$ (531 eV). Note that due to the higher excitation energy, the interference effect is smaller in this case and the plasmon contribution is larger than that in (a) (see Refs. 10 and 11).

figures, the total intensity is given by curves *a* which contain contributions of both Eqs. (30') and (31'). The contribution of Eq. (30') is given by curves *b* and that of Eq. (31') by curves *c* and *d*. In calculating the contribution of Eq. (31') we have separated the contributions related to the single-pair part and the plasmon part of $\text{Im}U_+(q, \omega)$. It is well known that the single-pair region of $\text{Im}U_+(q, \omega)$ is a two-dimensional region defined by $\max(0, q(q - 2k_F)) < 2m\omega < q(q + 2k_F)$. The other nonzero region is the one-dimensional plasmon region given by the plasmon dispersion curve $\omega_p(q)$ with $q < q_c$. We have first attempted to compute the contribution of Eq. (31') by making a simplification in which I^s is replaced by a δ function. This gives curve *c* for the single-pair contribution and curve *d'* for the plasmon contribution. This simplification is quite satisfactory for the single-pair curve

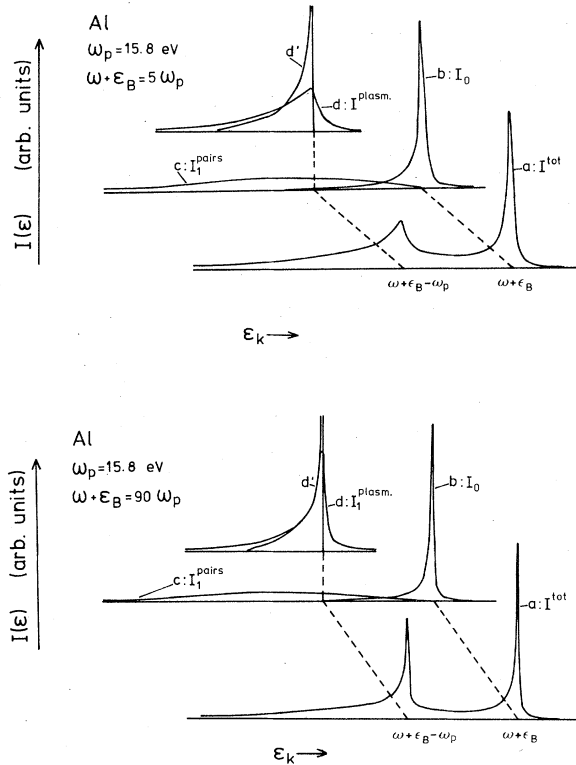


FIG. 6. (a) x-ray photoemission intensity in the main line and the first plasmon satellite regions in Al for the excitation energy of $5\omega_p$ (78.9 eV). (b) x-ray photoemission intensity of Al for the incident photon energy of $90\omega_p$ (1420 eV). In this case also the plasmon satellite has larger intensity due to smaller interference effect (see Refs. 10 and 11).

c which is smooth and which extends over a large region. However, for the plasmon curve d' , this replacement is not suitable since it gives rise to a singularity. Thus the plasmon calculation has to be carried out by keeping I^s in Eq. (31'). In other words, the intensity represented by curve d' has to be convoluted with intensity I^s to obtain the correct intensity which is given by curve d . The total intensity a is then obtained by summing contributions of curves b , c , and d .

Let us now make a digression of the method of our calculation of the intensity and the shape of the XPS of simple metals. Our calculation has been carried out in the RPA, where the effective electron-electron interaction \mathcal{U} has been divided into two parts [see Eq. (2)]. A part V , shown in Fig. 2, contains the static part of the potential (screened Coulomb potential) as well as the one-pair contribution of the dynamic part. This V part is a good approximation of \mathcal{U} for short distances and low-energy transfers (low-energy pair creation). The second part U , which merely

corresponds to the difference between \mathcal{U} and V , describes higher-energy transfer (high-energy pair creation), as well as the plasmon excitation in the electron gas.

The V part has been used to describe the ND-DS infrared catastrophe. Our treatment is in formal agreement with the ND-DS calculations. For $\epsilon \sim 0$ we have the XPS intensity given by a power law where the exponent depends on the Born phase shifts. This exponent given by¹⁵ $\alpha = \frac{1}{2}(1 + \pi a_B k_F)^{-1}$ can then be considered to be quite satisfactory as the numerical values (0.199 for Na and 0.128 for Al) agree within a few percent with the results obtained by much more elaborate methods.¹⁹ For larger ϵ our result, which is integrable, is still better than those of DS, which give a nonintegrable intensity at these energies.

We also introduce a linewidth in our calculation which is essentially related to the photoelectron damping. This is the only effect which modifies the line shape given by curves a (in Figs. 5 and 6) as the excitation energy $\omega + \epsilon_B$ varies. This width is roughly proportional to $(\omega + \epsilon_B)^{-1/2}$, and this explains why the calculated and the observed widths increase in the ultrasoft -XPS region. Note that

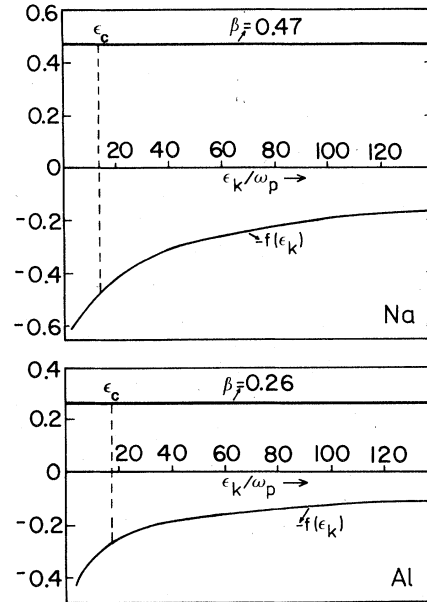


FIG. 7. Evolution of the interference term $-f(\epsilon_k)$ and the constant intrinsic term β appearing in Eq. (31) as a function of energy in Na and Al. The dashed vertical lines indicate the kinetic energy of the photoelectrons at which the total cancellation of these two terms occurs. This energy, where the XPS spectrum becomes similar to electron-energy-loss spectrum, is slightly higher than that calculated in Ref. 17 (see text).

the functions $\alpha(\epsilon)$ and $\xi_0(\epsilon)$ given by Eqs. (16) and (17) do not really depend upon the excitation energy.

The U part of the potential which is related to the high-energy pair production and plasmon excitation also introduces significant change in the intensity and the shape of the spectrum in the ultrasoft-XPS regime. The plasmon satellite and the background are significantly reduced in this regime principally due to the presence of the interference term (Eq. 26b) in the transition matrix element. This negative interference term which was first calculated by Chang and Langreth⁴ in a lowest-order perturbative expansion for high energies (>300 eV) and then extended by Chastenet and Longe¹⁷ to low energies, is also roughly proportional to $(\omega + \epsilon_B)^{-1/2}$. In Figs. 7 we show the evolution of our interference term and the intrinsic term as a function of the incident photon energy. These curves are very similar to those proposed by Chastenet and Longe, the slight difference being due to the fact that in the present paper we have incorporated the dispersion and the attenuation of the plasmon mode as q tends to q_c . Note that the intrinsic term remains practically constant whereas the interference term becomes more negative at lower excitation energies. The energy at which these two terms cancel each other is represented by ϵ_c . The high-

energy pair-production term which contributes to the background (curves c in Figs. 5 and 6) also shows similar behavior. The increase in the magnitude of the interference term at low energies can be interpreted quite easily. For slow photoelectrons, the intrinsic and the extrinsic productions occur practically in the same region of space, e.g., in the neighborhood of the ion which emits the photoelectron. Thus the interference is strongest at these low energies.^{10,11}

Finally, we would like to point out that the shape and size of the main line and the first plasmon satellite of the XPS of simple metals that we have calculated in this paper are very similar to the ones that have been experimentally observed by Williams *et al.*⁸ and more recently by Norman and Woodruff.⁹ To our knowledge this is the first theory which is truly unified in the sense that the same theory can calculate the asymmetry of the main line, the plasmon satellite, as well as the background of the XPS.

ACKNOWLEDGMENT

This research has been supported in part by the NATO Research Grant No. 1433, and in part by the Institut Interuniversitaire des Sciences Nucléaires, Belgium.

¹B. I. Lundqvist, Phys. Kondens. Mater. **9**, 236 (1969).

²S. Doniach and M. Šunjič, J. Phys. C **3**, 285 (1970).

³D. C. Langreth, Phys. Rev. B **1**, 471 (1970).

⁴J. J. Chang and D. C. Langreth, Phys. Rev. B **5**, 3512 (1972); D. C. Langreth, in *Collective Properties of Physical Systems*, 24th Nobel Symposium, edited by B. I. Lundqvist and S. Lundqvist (Academic, New York, 1974), p. 210.

⁵A. A. Lucas and M. Šunjič, Prog. Surf. Sci. **2**, 75 (1972); M. Šunjič and D. Šokčević, J. Electron. Spectrosc. Relat. Phenom. **5**, 936 (1974).

⁶W. J. Pardee, G. D. Mahan, D. E. Eastman, R. A. Pollak, L. Ley, F. R. McFeely, S. P. Kowalczyk, and D. A. Shirley, Phys. Rev. B **11**, 3614 (1975).

⁷D. R. Penn, Phys. Rev. Lett. **38**, 1429 (1977); *ibid.* **40**, 568 (1978).

⁸R. S. Williams, P. S. Wehner, G. Apai, J. Stohr, D. A. Shirley, and S. P. Kowalczyk, J. Electron. Spectrosc. Relat. Phenom. **12**, 477 (1977).

⁹D. Norman and D. P. Woodruff, Surf. Sci. **79**, 76 (1979).

¹⁰S. A. Flodstrom, R. Z. Bachrach, R. S. Bauer, J. C. McMenamin, and S. B. M. Hagstrom, J. Vac. Sci. Technol. **14**, 303 (1977).

¹¹L. I. Johansson and I. Lindau, Solid State Commun. **29**, 379 (1979).

¹²S. M. Bose and P. Longe, Phys. Rev. B **18**, 3921 (1978); C. Sénémaud, *ibid.* **18**, 3929 (1978).

¹³J. J. Chang and D. C. Langreth, Phys. Rev. B **8**, 4638 (1973).

¹⁴P. Nozières and C. T. deDominicis, Phys. Rev. **178**, 1097 (1969).

¹⁵P. Longe, Phys. Rev. B **8**, 2572 (1973).

¹⁶B. Bergersen, F. Brouers, and P. Longe, J. Phys. F **1**, 945 (1971); Solid St. Commun. **8**, 1423 (1970).

¹⁷D. Chastenet and P. Longe, Phys. Rev. Lett. **44**, 91 (1980); **44**, 903(E) (1980).

¹⁸P. Longe and A. J. Glick, Phys. Rev. **177**, 526 (1969).

¹⁹G. A. Ausman and A. J. Glick, Phys. Rev. **183**, 687 (1969).